Cancer Research

CBP Loss Cooperates with PTEN Haploinsufficiency to Drive Prostate Cancer: Implications for Epigenetic Therapy

Liya Ding[1,2,4], Shuai Chen[6], Ping Liu[6,10], Yunqian Pan[1,2,4], Jian Zhong[1,2,4], Kevin M. Regan[2], Liguo Wang[3], Chunrong Yu[8], Anthony Rizzardi[7], Liang Cheng[9], Jun Zhang[5], Stephen C. Schmechel[7], John C. Cheville[5], Jan Van Deursen[1,4], Donald J. Tindall[2,4], and Haojie Huang[1,2,4]

Abstract

Despite the high incidence and mortality of prostate cancer, the etiology of this disease is not fully understood. In this study, we develop functional evidence for CBP and PTEN interaction in prostate cancer based on findings of their correlate expression in the human disease. *Cbp*$^{pc-/-}$;*Pten*$^{pc+/-}$ mice exhibited higher cell proliferation in the prostate and an early onset of high-grade prostatic intraepithelial neoplasia. Levels of EZH2 methyltransferase were increased along with its Thr350 phosphorylation in both mouse Cbp$^{-/-}$; Pten$^{+/-}$ and human prostate cancer cells. CBP loss and PTEN deficiency cooperated to trigger a switch from K27-acetylated histone H3 to K27-trimethylated bulk histones in a manner associated with decreased expression of the growth inhibitory EZH2 target genes *DAB2IP*, *p27*^{KIP1}, and *p21*^{CIP1}. Conversely, treatment with the histone deacetylase inhibitor panobinostat reversed this switch, in a manner associated with tumor suppression in *Cbp*$^{pc-/-}$;*Pten*$^{pc+/-}$ mice. Our findings show how CBP and PTEN interact to mediate tumor suppression in the prostate, establishing a central role for histone modification in the etiology of prostate cancer and providing a rationale for clinical evaluation of epigenetic-targeted therapy in patients with prostate cancer. *Cancer Res; 74(7); 2050–61. ©2014 AACR.*

Introduction

Prostate cancer is the most commonly diagnosed malignancy and the second leading cause of cancer death in American men. Clinical prostate cancer is extremely rare in men younger than 45 years of age, with less than 1 in 10,000 occurrences. The incidence increases dramatically over the ensuing decades, with a 1 in 6 chance of cancer detection between the ages of 60–80. Intriguingly, autopsy studies demonstrate that high-grade prostatic intraepithelial neoplasia (PIN) and small/microscopic carcinomas are present in the prostate of up to 29% of men at 30 to 40 years of age (1). These findings indicate that PIN/low-grade cancers frequently develop in the prostate of adult men at an early age. It is of paramount importance to elucidate the genetic/epigenetic lesions responsible for early-stage pathogenesis in the prostate.

The tumor suppressor gene *PTEN* is frequently mutated, deleted, or expressed at reduced levels in human prostate cancer (2, 3). Loss of heterozygosity (LOH) in the *PTEN* locus occurs in up to 20% of localized but more than 60% of advanced/metastatic prostate cancer, suggesting that *PTEN* haploinsufficiency plays an important role in prostate cancer initiation and development into the advanced/aggressive stage. Mouse genetic studies show that *Pten* heterozygous deletion alone fails to induce high-grade PIN until mice are older than 12 months (4, 5), suggesting that monoallelic loss of *PTEN* is insufficient to initiate prostate neoplasia and that cooperating oncogenic alterations are required.

CBP (CREB-binding protein, CREBBP) is a histone acetyltransferase that participates in many biologic processes, including cell growth, transformation, and organ development (6). Genome-wide analyses of histone modification show that histone acetylation generally correlates with gene activation (7), which is consistent with the finding that both mammalian and *Drosophila* CBP are involved in gene transactivation by mediating histone H3 lysine 27 acetylation (H3K27Ac; refs. 8, 9). Gene inactivation mutations and chromosomal translocations with breakpoints at the *CBP* gene locus are frequently detected in different types of hematologic malignancies, including acute lymphoblastic

Authors' Affiliations: Departments of [1]Biochemistry and Molecular Biology, [2]Urology, and [3]Biomedical Statistics and Informatics, [4]Mayo Clinic Cancer Center, and [5]Department of Laboratory Medicine and Pathology, Mayo Clinic College of Medicine, Rochester; [6]Masonic Cancer Center; [7]Department of Laboratory Medicine and Pathology, University of Minnesota, Minneapolis, Minnesota; [8]Astar Biotech LLC, Richmond, Virginia; [9]Department of Pathology and Laboratory Medicine, Indiana University School of Medicine, Indianapolis, Indiana; and [10]College of Life Sciences, Nanjing Normal University, Nanjing, China

Note: Supplementary data for this article are available at Cancer Research Online (http://cancerres.aacrjournals.org/).

L. Ding and S. Chen contributed equally to this work.

Current address for A. Rizzardi and S.C. Schmechel: Department of Pathology, University of Washington, Seattle, Washington.

Corresponding Author: Haojie Huang, Mayo Clinic, 200 First Street SW, Rochester, MN 55905. Phone: 507-293-1712; Fax: 507-293-3071; E-mail: huang.haojie@mayo.edu.

doi: 10.1158/0008-5472.CAN-13-1659

leukemia and B-cell lymphoma (10, 11). Mouse genetic studies show that thymocyte-specific *CBP* deletion causes T-cell lymphoma (12). These findings imply that CBP functions as a hematologic tumor suppressor. Moreover, LOH at the *CBP* locus has been reported in human solid tumors and cancer cell lines, including PC-3 prostate cancer cells (13, 14). However, the relevance and the exact role of CBP in prostate cancer pathogenesis are not fully understood. In the present study, we demonstrate that reduced expression of CBP correlates with PTEN expression in a cohort of human prostate tumors. Concomitant deletion of *Cbp* and *Pten* induces early-life high-grade PIN/low-grade cancer. Treatment of *Cbp*/*Pten* compound-deficient mice with the histone deacetylase inhibitor panobinostat diminishes PIN lesions.

Materials and Methods

Generation of *Cbp* and *Pten* prostate-specific deletion mice

Cbp conditional knockout ($Cbp^{L/L}$) mice were provided by Dr. Jan van Deursen at Mayo Clinic (12). *Pten* conditional knockout ($Pten^{L/L}$) mice were originally generated in the laboratory of Dr. Hong Wu at University of California Los Angeles (Los Angeles, CA; ref. 15) and purchased from The Jackson Laboratory. *Pb-Cre4* transgenic mice generated in the laboratory of Dr. Pradip Roy-Burman at University of Southern California, Los Angeles, CA (16) were acquired from the National Cancer Institute (NCI) Mouse Repository. Cohorts of $Cbp^{pc-/-}$;$Pten^{pc+/-}$, $Cbp^{L/L}$;$Pten^{L/+}$, $Cbp^{pc-/-}$ and $Pten^{pc+/-}$ mice were generated from $Cbp^{pc+/-}$;$Pten^{pc+/-}$ males and $Cbp^{L/+}$;$Pten^{L/+}$ females, which were obtained by cross breeding *Pb-Cre4* males with $Cbp^{L/L}$ and $Pten^{L/L}$ females. All mice were maintained under standard conditions of feeding, light, and temperature with free access to food and water. All experimental protocols were approved by the Institutional Animal Care and Use Committee at Mayo Clinic.

PCR-based genotyping of mice

Genotyping of wild-type and conditional alleles of *Cbp* and *Pten* genes as well as the *Cre* transgene was performed according to previously described PCR protocols (12, 16, 17). Primer sequences are provided in Supplementary Table S1.

Cell lines, cell culture, and transfection

DU145 cell line was purchased from the American Type Culture Collection and cultured in RPMI-1640 (Invitrogen) supplemented with 10% FBS (Hyclone). LAPC-4 cell line was provided by Dr. Charles Sawyers (Memorial Sloan-Kettering Cancer Center, New York, NY) and cultured in Iscove's Modified Eagle Medium (IMEM) with 10% FBS. *Pten*-positive and -negative MEFs were provided by Dr. Zhenbang Chen at Meharry Medical College (Nashville, TN; ref. 18) and cultured in Dulbecco's Modified Eagle Medium with 10% FBS. These cell lines have been tested and authenticated (karyotyping, AR expression, and PTEN mutation status) for less than 6 months before the first submission of the manuscript. Cell transfection was performed by electroporation using an Electro Square Porator ECM 830 (BTX) as described previously (19).

Panobinostat (LBH589) treatment of mice

Six-month-old $Cbp^{pc-/-}$;$Pten^{pc+/-}$ male mice were randomly assigned into two groups ($n = 9$/group) for treatment with vehicle or LBH589 (20 mg/kg/d) daily by intraperitoneal injection for 30 days. LBH589 was dissolved in 5% DMSO/PBS solution.

Human prostate cancer specimens, tissue microarray construction, and immunohistochemistry

Three intermediate-density prostate cancer TMAs were prepared by the Tissue and Cell Molecular Analysis Shared Resource at the Mayo Clinic Cancer Center. These TMAs contain cancerous (Gleason sum 4–9) and tumor-adjacent benign tissues from the radical prostatectomy specimens of 78 patients with clinically localized prostate cancer (approximately four cores per case). All cases upon collection into the resource (approved by the Mayo Clinic Institutional Review Board) had repeat pathology characterization of tissues and review of medical records. IHC of TMA slides with antibodies for CBP, PTEN, and $p27^{KIP1}$ were performed as described in Supplementary Information. Digital images of IHC-stained TMA slides were obtained at ×40 magnification (0.0625 μm^2/raw image pixel) using a whole slide scanner (ScanScope CS, Aperio).

Statistical Analysis

Cell culture experiments were carried out with three or more replicates. Statistical analyses were performed by the Student *t* test for cell culture and mouse tissue studies. The Fisher exact test (right tail) was used to measure the association of the expression of CBP, PTEN, and $p27^{KIP1}$ proteins in human prostate cancer specimens. *P* values of <0.05 are considered significant.

Additional methods

Additional methods are provided in Supplementary Information.

Results

Expression of CBP and PTEN protein correlates in human prostate cancer specimens

mRNA-based analysis shows that *CBP* expression appears to be lower in prostate cancers than in benign prostatic hyperplasias (20). An independent IHC study demonstrates that the CBP protein is well expressed in both normal and malignant human prostate tissues (21). Notably, CBP expression is completely lost in a subset of primary tumors and lymph node metastases, but not in any benign prostate tissues examined (21). Because the previous findings regarding CBP expression in human prostate cancers are not entirely consistent, we employed TMA and IHC approaches to examine CBP protein expression in a cohort of human prostate cancers ($n = 271$ TMA specimens) and tumor-adjacent benign tissues ($n = 25$ TMA elements) obtained from 78 patients. IHC staining was evaluated on the basis of a semi-quantitative scale by considering both percentage of positive cells and staining intensity. We found that approximately 80% of benign tissues, but only about 45% of cancers expressed higher levels (staining index

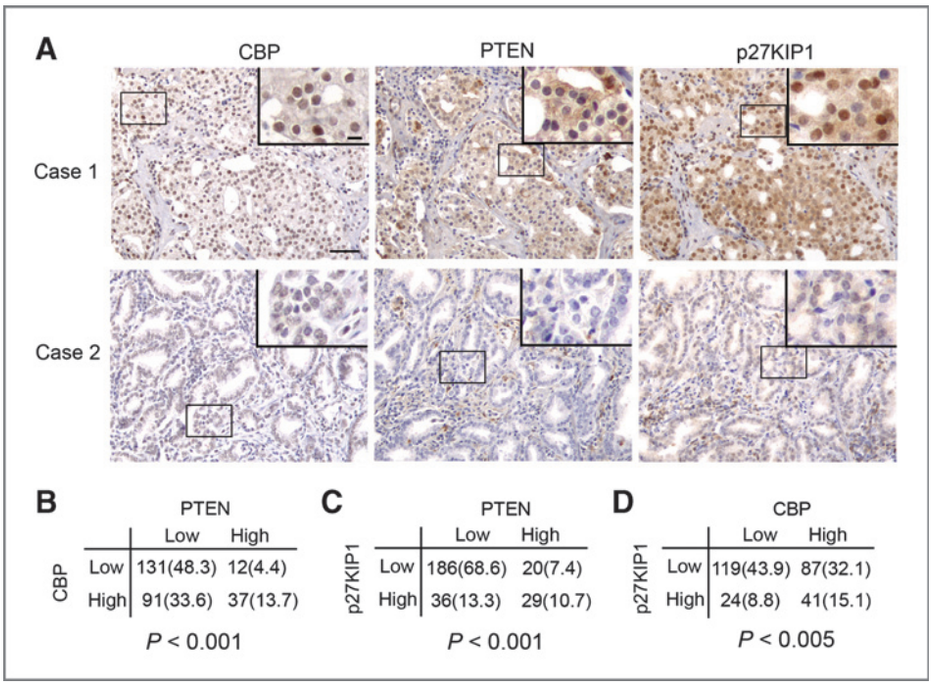

Figure 1. Correlation of CBP, PTEN, and $p27^{KIP1}$ protein expression in human prostate cancer. A, representative images of prostate tumors exhibiting high and low expression of CBP, PTEN, and $p27^{KIP1}$ proteins, respectively. Scale bar, 50 μm. Insets show high magnification images; scale bar, 10 μm. B–D, proportions of human prostate cancers ($n = 271$ TMA elements) that show high (SI score > 4) or low (SI score ≤ 4) expression of CBP, PTEN, and $p27^{KIP1}$ proteins. The correlation between PTEN and CBP, PTEN and $p27^{KIP1}$, and CBP and $p27^{KIP1}$ expression was observed, as determined by the Fisher exact test (right tail). The number in parentheses is the percentage of the number of cases in each category over the number of total cases examined.

(SI) ≥ 6 of CBP protein; Supplementary Fig. S1A). Moreover, approximately 20% of cancers, but not benign tissues expressed none or low levels (SI < 3) of CBP protein. Representative images of CBP staining in benign and cancerous tissues are shown in Supplementary Fig. S1B. Statistical analysis of the quantitative data confirmed that CBP expression was significantly lower in cancers than in benign tissues (Supplementary Fig. S1C). IHC analysis in an additional cohort of 20 non-TMA specimens demonstrated that CBP protein level was significantly lower in PIN lesions than that in the adjacent benign tissues (Supplementary Fig. S2).

Because partial loss of *PTEN* is fairly common in human prostate cancer (3, 22) and yet requires cooperating oncogenic lesions in prostate oncogenesis (4, 23), we examined PTEN expression in the cohort of TMA specimens and sought to determine whether the expression of CBP and PTEN protein correlates in these patients. Representative images of high and low staining of CBP and PTEN are shown in the top and bottom panels of Fig. 1A, respectively. The Fisher exact test demonstrated that reduced expression of CBP and PTEN protein correlates in 271 TMA prostate cancer specimens (Fig. 1B). Expression of these proteins also correlates with $p27^{KIP1}$, a common downstream target of them (see details below) in this cohort of specimens (Fig. 1A, C, and D).

CBP and PTEN act synergistically in prostate cell proliferation and tumor formation

To explore the role of CBP in prostate cancer pathogenesis, we crossed *Cbp* conditional ($Cbp^{Loxp/Loxp}$, hereafter termed as $Cbp^{L/L}$) mice (12) with *probasin* (*Pb*)-*Cre* transgenic mice (*Pb-Cre4*) that express Cre recombinase in prostate epithelial cells (16). Effective deletion of the *Cbp* gene and protein was detected by PCR and immunofluorescent cytochemistry, respectively, in *Pb-Cre4*;$Cbp^{L/+}$ ($Cbp^{pc+/-}$) and *Pb-Cre4*;$Cbp^{L/L}$ (hereafter termed as $Cbp^{pc-/-}$) mice (Supplementary Figs. S3A and S3B and S4A). Similar to the *Cre*-negative control mice, no signs of pathology were detected in all lobes of the prostate, including anterior prostate (AP), dorsolateral prostate (DLP), and ventral prostate (VP), in $Cbp^{pc-/-}$ mice within 12 months of age (Fig. 2A and Supplementary Fig. S4B), indicating that cooperative oncogenic lesions are required. Because the TMA data showed that reduced expression of CBP and PTEN proteins correlates in human prostate cancer specimens (Fig. 1B), we sought to determine whether concomitant deletion of *Cbp* and *Pten* genes accelerates prostate cancer formation in mice. We established cohorts of $Cbp^{L/L}$;$Pten^{L/+}$ (Cre-negative control), $Cbp^{pc-/-}$, $Pten^{pc+/-}$ and $Cbp^{pc-/-}$;$Pten^{pc+/-}$ males by intercrossing *Pb-Cre4*, $Cbp^{L/L}$ and $Pten^{L/L}$ (15) mice. PCR-based analysis demonstrated that the *Cbp* gene was almost completely deleted, but the *Pten* gene was only partially deleted in all the lobes of the prostates in $Cbp^{pc-/-}$;$Pten^{pc+/-}$ mice (Supplementary Fig. S3C). As early as 4 months of age, more than 80% of $Cbp^{pc-/-}$;$Pten^{pc+/-}$ mice ($n = 11$) exhibited clear histologic evidence of low-grade PIN (mouse PIN I and II) in all lobes, including AP, DLP, and VP (Supplementary Table S2). At 6 months of age, focal high-grade PIN (mouse PIN III and IV) in AP and DLP and low-grade PIN (mouse PIN II) in VP were detected in 100% penetrance in $Cbp^{pc-/-}$;$Pten^{pc+/-}$ mice examined ($n = 20$; Fig. 2A and Supplementary Fig. S4B; Supplementary Table S2). In contrast, no PIN was detected in the prostates of all $Cbp^{pc-/-}$ littermates examined at this age ($n = 15$; Fig. 2A and Supplementary Table S2). Similar to the earlier reports that approximately 10% of *Pten* heterozygous mice develop PIN at an age younger than 9 months (4, 5), low-grade PIN was observed in only 1 of 12 $Pten^{pc+/-}$ males and no PIN was detected in the other 11 $Pten^{pc+/-}$ mice at 6 months of age

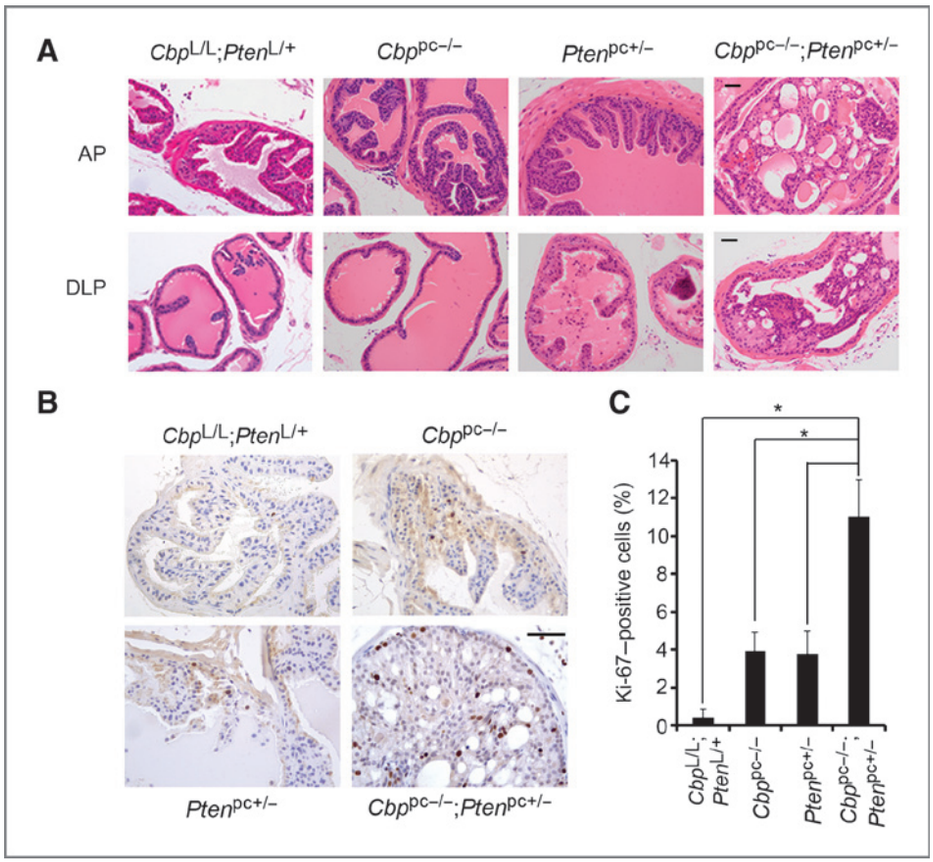

Figure 2. Concomitant deletion of two *Cbp* alleles and one *Pten* allele induces high-grade PIN and enhances prostatic epithelial cell proliferation. A, H&E of anterior (AP) and dorsolateral (DLP) prostates of 6-month-old $Cbp^{L/L};Pten^{L/+}$ (wild-type), $Cbp^{pc-/-}$, $Pten^{pc+/-}$, and $Cbp^{pc-/-};Pten^{pc+/-}$ mice. Scale bar, 50 μm. B and C, Ki-67 staining analysis in the prostates of 6-month-old $Cbp^{L/L};Pten^{L/+}$, $Cbp^{pc-/-}$, $Pten^{pc+/-}$, and $Cbp^{pc-/-};Pten^{pc+/-}$ mice. Representative images of Ki-67 staining in each genotype are shown in B and quantitative data are shown in C. Scale bar, 50 μm. *, $P < 0.01$.

(Fig. 2A and Supplementary Table S2). No neoplastic changes were detected in any $Cbp^{L/L};Pten^{L/+}$ control mice ($n = 16$) (Fig. 2A and Supplementary Table S2). These histologic data indicate that loss of *CBP* cooperates with *PTEN* haploinsufficiency in prostate tumorigenesis. Accordingly, Ki-67 staining significantly increased in $Cbp^{pc-/-};Pten^{pc+/-}$ prostates compared with $Cbp^{L/L};Pten^{L/+}$, $Cbp^{pc-/-}$, or $Pten^{pc+/-}$ counterparts (Fig. 2B and C), suggesting that combined inactivation of *CBP* and *PTEN* promotes prostate epithelial cell proliferation *in vivo*.

Coregulation of $p27^{KIP1}$ and DAB2IP expression by CBP and PTEN *in vitro* and *in vivo*

To explore the molecular mechanism underlying CBP/PTEN deletion-induced prostate cancer cell proliferation, we used small interfering RNAs (siRNA) to knock down endogenous CBP and PTEN individually or in combination in PTEN-positive human prostate cancer cell lines and measured the impact on cell-cycle control. Concomitant knockdown of CBP and PTEN increased proliferation of DU145 cells (Fig. 3A and B), although the effect was not as robust as in *Cbp*/*Pten* knockout mice (Fig. 2B and C). Knockdown of CBP and PTEN either alone or in combination had little or no effect on expression of several key cell-cycle–driven proteins, including CDK1, CDK2, CDK6, and cyclin B1, with an exception of cyclin D1 (Fig. 3B). In contrast, CBP and/or PTEN knockdown markedly decreased the expression of the CDK inhibitors $p27^{KIP1}$ and $p21^{CIP1}$ and the growth-inhibitory protein DAB2IP, expression of which is often downregulated in human prostate cancer (Fig. 3B; refs. 24, 25). CBP and/or PTEN knockdown also downregulated expression of $p27^{KIP1}$, $p21^{CIP1}$, and *DAB2IP* mRNAs in DU145 cells (Fig. 3C). Similar results were obtained in LAPC-4 cells (Supplementary Fig. S5A and B).

Next, we examined the impact of *Cbp* and *Pten* deletion on expression of $p27^{Kip1}$, $p21^{Cip1}$, and Dab2ip proteins in the mouse prostate. Nuclear expression of Cbp protein, nuclear, and cytoplasmic expression of Pten protein and no expression of phosphorylated Akt (Akt-p) was observed in prostate epithelial cells of $Cbp^{L/L};Pten^{L/+}$ control mice (Fig. 4A–D, left). As expected, Pten expression was reduced in the noncancerous prostate epithelium in $Cbp^{pc-/-};Pten^{pc+/-}$ mice (Fig. 4C, middle), but surprisingly Pten protein was hardly detected in PIN lesions in the same mice (Fig. 4C, right). Accordingly, Akt-p was robustly elevated in PIN, but not in the adjacent normal epithelium in $Cbp^{pc-/-};Pten^{pc+/-}$ mice (Fig. 4D, middle and right). $P27^{Kip1}$ and Dab2ip proteins were well expressed in both cytoplasm and nucleus in the normal prostate epithelium of control mice (Fig. 4E and F, left). Consistent with decreased expression of Cbp and Pten and increased expression of Akt-p, there were less cells expressing $p27^{Kip1}$ and Dab2ip proteins in PIN lesions in $Cbp^{pc-/-};Pten^{pc+/-}$ mice than in the normal prostates of control littermates (Fig. 4E and F, right). The specificity of the antibodies for $p27^{Kip1}$ and Dab2ip proteins

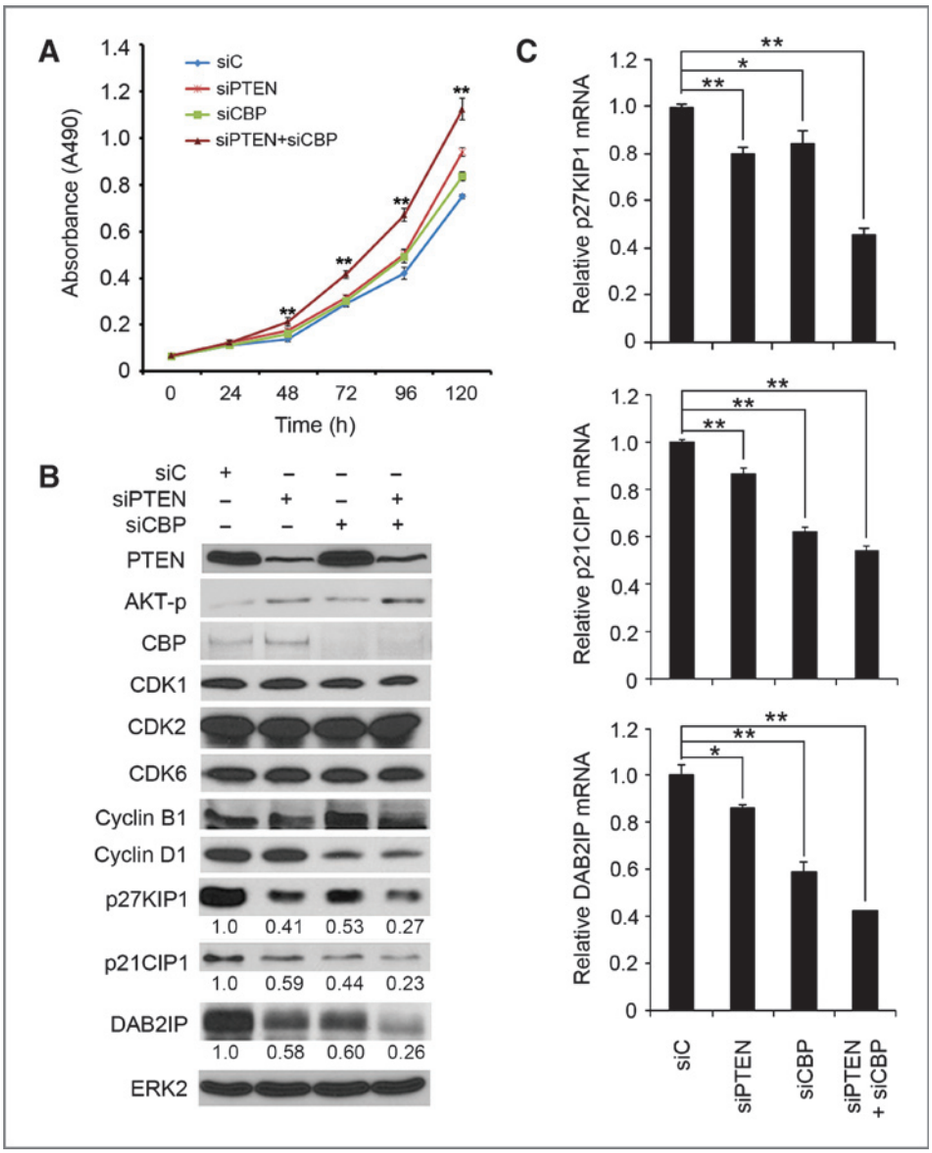

Figure 3. Effect of CBP and PTEN knockdown on human prostate cancer cell proliferation and expression of cell cycle-regulatory genes. A, DU145 prostate cancer cells were transfected as indicated and then seeded into 96-well plates for MTS assays. Data are means ± SD from experiments with four replicates ($n = 4$). **, $P < 0.01$, comparing siPTEN+siCBP group with siC group. B, DU145 cells were transfected as in A for 48 hours followed by Western blot analyses. The density of $p27^{KIP1}$, $p21^{CIP1}$, and DAB2IP was determined by normalizing to ERK2 (loading control) first and then to the normalized value in siC-transfected cells. C, DU145 cells were transfected as in A for 36 hours followed by RT-qPCR analysis. Data, means ± SD. from experiments with three replicates ($n = 3$). **, $P < 0.01$ and *, $P < 0.05$.

were demonstrated by siRNA knockdown and IHC assays (Supplementary Fig. S6A and S6B). The IHC staining for Cbp, Pten, Akt-p, $p27^{Kip1}$, and Dab2ip was quantified and the data are shown in Supplementary Fig. S7. Despite multiple efforts, we were unable to validate an antibody that can effectively detect $p21^{Cip1}$ protein in mouse prostate sections by IHC. We conclude that knockdown or knockout of CBP and PTEN inhibits expression of $p27^{KIP1}$, $p21^{CIP1}$, and DAB2IP in human prostate cancer cells and $p27^{Kip1}$ and Dab2ip expression in the mouse prostate. Moreover, $p27^{KIP1}$ is a known tumor suppressor that is often downregulated in human prostate cancer (26). IHC staining and correlation studies showed that reduced expression of $p27^{KIP1}$ correlates with CBP and PTEN expression in the cohort of 271 TMA specimens of human prostate cancer (Fig. 1A, C, and D). These data suggest that expression of $p27^{KIP1}$ protein may also be regulated by CBP and/or PTEN in human prostate cancer.

CBP and PTEN regulation of H3K27Ac and H3K27me3 in human and mouse prostate cancer cells

CBP as a histone acetyltransferase responds for the "open" chromatin mark histone H3 lysine 27 acetylation (H3K27Ac) and gene activation in mammals and flies (8, 27, 28). In contrast, the histone methyltransferase EZH2 mediates the "close" chromatin mark H3 lysine 27 trimethylation (H3K27me3) and gene repression (29). It has been shown recently that CDK-dependent phosphorylation of EZH2 at threonine 350 (T350-p) is important for EZH2-mediated H3K27me3 and gene repression (19, 30, 31). Consistent with the report that PTEN inactivation increases CDK enzymatic activity and promotes cell-cycle progression (32), we found that *Pten* homozygous deletion in MEF or knockdown in DU145 human prostate cancer cells increases the overall levels of T350 (T345 in mouse) phosphorylated EZH2 and H3K27me3 levels (Fig. 5A and B). PTEN inactivation also increased total

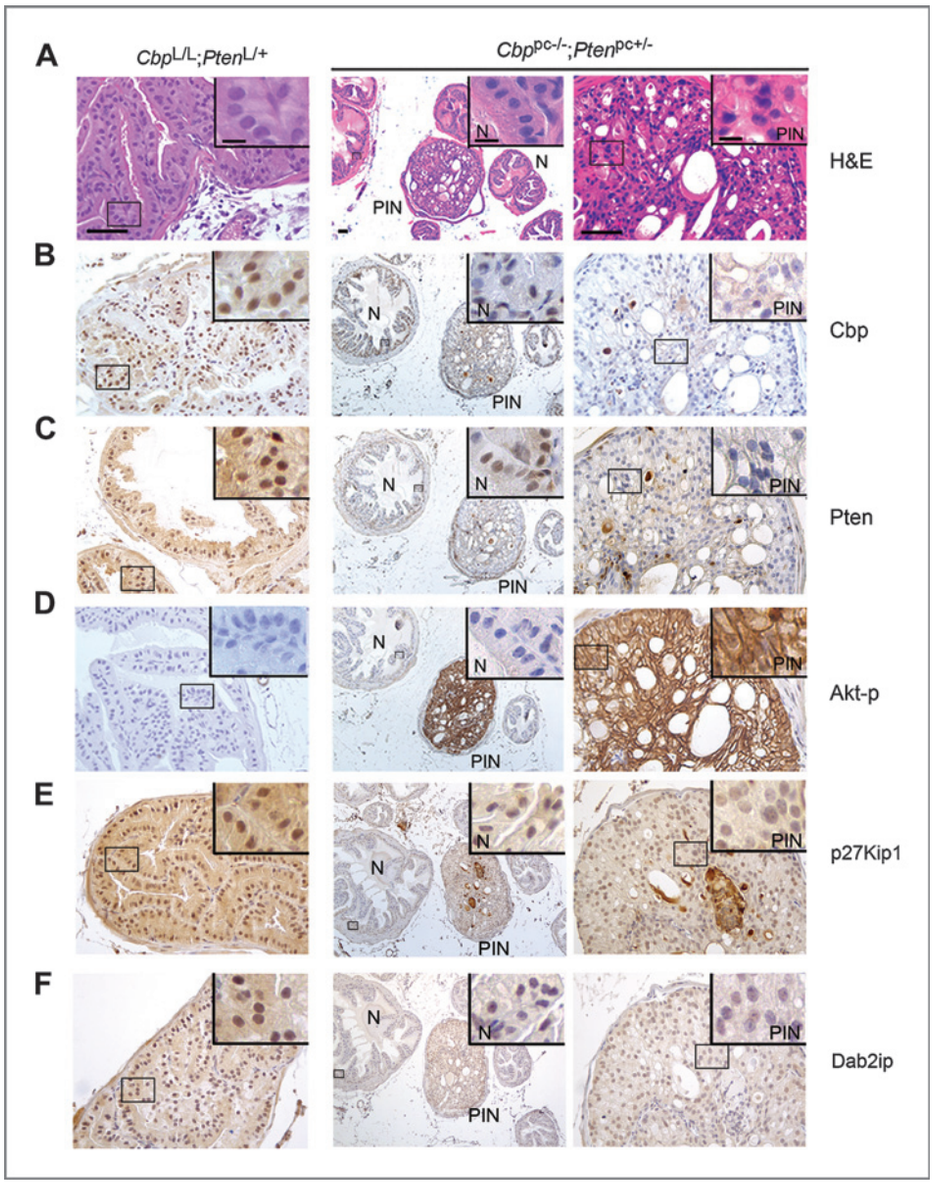

Figure 4. Immunohistochemical analysis of protein expression in prostate sections of *Cbp*/*Pten*-deficient and "wild-type" mice. A, H&E of prostate sections of 6-month-old $Cbp^{L/L};Pten^{L/+}$ and $Cbp^{pc-/-};Pten^{pc+/-}$ mice. Scale bar, 50 μm. Insets show high magnification images; scale bar, 10 μm. N, normal; PIN, prostatic intraepithelial neoplasia. B–F, immunohistochemical analysis of prostate sections of 6-month-old $Cbp^{L/L};Pten^{L/+}$ and $Cbp^{pc-/-};Pten^{pc+/-}$ mice for expression of Cbp (B), Pten (C), Akt-p (serine 473 phosphorylation; D), $p27^{Kip1}$ (E), and Dab2ip (F).

EZH2 levels in both MEF and DU145 cells (Fig. 5A and B), which is consistent with early reports that EZH2 protein and mRNA are upregulated in prostate cancers in $Nkx3.1^{+/-};Pten^{+/-}$ compound and $Pten^{pc-/-}$ mice (33, 34). Accordingly, CBP and PTEN knockdown alone or together resulted in concomitant upregulation of H3K27me3 and downregulation of H3K27Ac, an H3K27Ac-to-H3K27me3 switch in bulk histones in both DU145 and LAPC-4 cell lines (Fig. 5C–E and Supplementary Fig. S5A). Moreover, we recently identified *Dab2ip*, $p27^{Kip1}$, and $p21^{Cip1}$ as Ezh2 targets in mouse embryonic stem cells (35) and this finding was confirmed by ChIP-qPCR in DU145 cells (Supplementary Fig. S8). Consistent with the changes in the overall levels of H3K27Ac and H3K27me3 (Fig. 5C–E), codepletion of PTEN and CBP resulted in concomitant increase in H3K27me3 (except the $p21^{CIP1}$ locus) and decrease in H3K27Ac at these gene loci in DU145 cells (Supplementary Fig. S9).

H3K27Ac levels were lower but H3K27me3 levels were much higher in PIN lesions in *Cbp*/*Pten* double knockout mice (Fig. 6A and B, right) compared with adjacent normal prostate epithelial cells in *Cbp*/*Pten*-deficient mice and normal prostate epithelium in control mice (Fig. 6A and B, middle and left). Accordingly, the levels of total and T345-phosphorylated Ezh2 were higher in *Cbp*/*Pten* double knockout PIN relative to adjacent normal prostate epithelium in both *Cbp*/*Pten* deficient and wild-type control mice (Fig. 6C and D). Although total Ezh2 levels markedly increased (Fig. 6C), the level of serine 21 phosphorylation (S21-p), which inhibits EZH2's H3K27me3 activity (36), was only modestly elevated in PIN compared with the adjacent noncancerous *Cbp*/*Pten*-deficient cells (Fig. 6E). The specificity of antibodies for EZH2, T350-p, S21-p, and H3K27me3 was demonstrated by siRNA knockdown and IHC assays (Supplementary Fig. S6C) or described previously

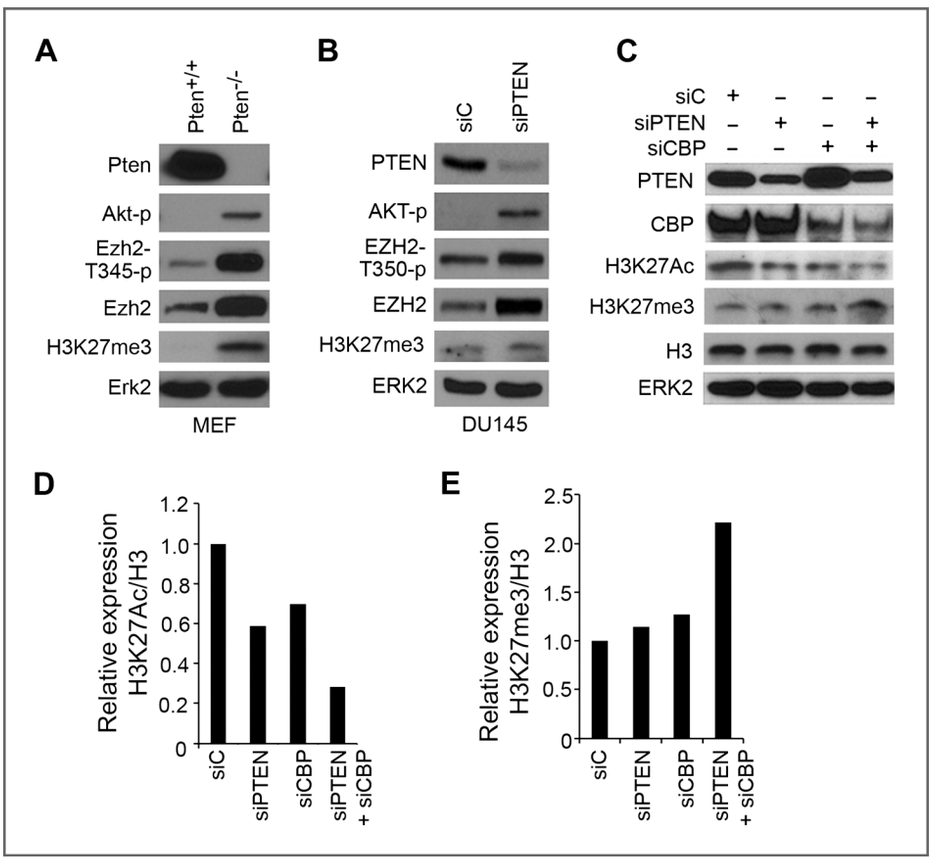

Figure 5. Effect of CBP and PTEN deficiency on expression of total and T350-phosphorylated EZH2, H3K27Ac and H3K27me3 levels on bulk histones. A, Western blot analysis of indicated proteins in Pten-proficient ($^{+/+}$) and -deficient ($^{-/-}$) MEFs. B, DU145 cells transfected as indicated for 48 hours followed by Western blot analysis. C–E, DU145 cells were transfected as indicated for 36 hours. Cytosolic (PTEN, ERK2) and nuclear (CBP, H3K27Ac, H3K27me3 and H3) extracts were prepared for Western blot (chemiluminescence-based) analysis of expression of indicated proteins (C). The relative expression of H3K27Ac and H3K27me3 was determined by normalizing to histone H3 first and then to the normalized value in siC-transfected cells and the quantitative data are shown in D and E, respectively. The experiments were repeated twice. Similar results were obtained from these experiments and the data shown was from one experiment.

(19, 36, 37). The quantified IHC data of H3K27Ac, H3K27me3, Ezh2, T345-p, and S21-p are shown in Supplementary Fig. S10. These data indicate that depletion of CBP and PTEN cooperatively induces a decrease in H3K27Ac and an increase in H3K27me3 in bulk histones in human prostate cancer cells and an H3K27Ac-to-H3K27me3 switch in the mouse prostate.

The histone deacetylase inhibitor panobinostat reverses neoplastic growth in *Cbp*/*Pten* deletion prostates in mice

Because of the competitive nature of H3K27Ac and H3K27me3 modifications on the same lysine residue and the H3K27Ac-to-H3K27me3 switch induced by CBP and PTEN knockdown or knockout, we sought to determine whether the treatment of *Cbp*/*Pten*-deficient tumors with the histone deacetylase (HDAC) inhibitor would reverse the H3K27Ac-to-H3K27me3 ratio and induce tumor repression. Cinnamic acid hydroxamate panobinostat (LBH589) inhibits classes I and II HDACs (38) and is currently being tested in clinical trials for various malignancies, including prostate cancer (39, 40). We, therefore, measured the therapeutic effect of LBH589 on prostate tumor growth in $Cbp^{pc-/-}$;$Pten^{pc+/-}$ mice. 6-month-old $Cbp^{pc-/-}$;$Pten^{pc+/-}$ mice were randomly assigned for treatment with vehicle or LBH589 (20 mg/kg body weight; $n = 9$/group). We found that LBH589 not only inhibited disease progression, but also induced tumor regression by decreasing the incidence of PIN lesions in *Cbp*/*Pten* knockout mice (Fig. 7A). Moreover, LBH589 treatment induced nuclear condensation, Akt phosphorylation (Akt-p) inhibition, increase in H3K27Ac, and decrease in H3K27me3 levels in the prostates of $Cbp^{pc-/-}$;$Pten^{pc+/-}$ mice (Fig. 7B). It has been shown recently that treatment of chondrocytes with SAHA, another HDAC inhibitor, increased expression of PHLPP1, a known AKT phosphatase (41). Similarly, we found that LBH589 treatment of DU145 cells resulted in a moderate increase in PHLPP1 expression (Supplementary Fig. S11A). These data suggest that panobinostat-induced inhibition of AKT phosphorylation can be attributed, at least in part, to PHLPP1 upregulation although our data cannot rule out other mechanisms of panobinostat action on AKT.

Further ChIP analysis showed that LBH589 treatment induced an increase in H3K27Ac and a decrease in H3K27me3 levels at *DAB2IP* and $p21^{CIP1}$ gene loci in CBP and PTEN coknockdown DU145 cells (Fig. 7C and Supplementary Fig. S11B). LBH589 also increased H3K27Ac but decreased H3K27me3 levels on bulk histones in CBP/PTEN double knockdown DU145 cells (Fig. 7D). Ki-67 staining and terminal deoxynucleotidyl transferase–mediated dUTP nick end labeling (TUNEL) assays demonstrated that treatment with LBH589 decreased cell proliferation and increased apoptosis in the prostates of $Cbp^{pc-/-}$;$Pten^{pc+/-}$ mice (Fig. 7E). The IHC staining for Akt-p, H3K27Ac, H3K27me3, Ki-67, and TUNEL staining was quantified and the data are shown in Supplementary Fig. S11C–S11G. The effect of LBH589 on apoptosis was further confirmed by its induction of changes

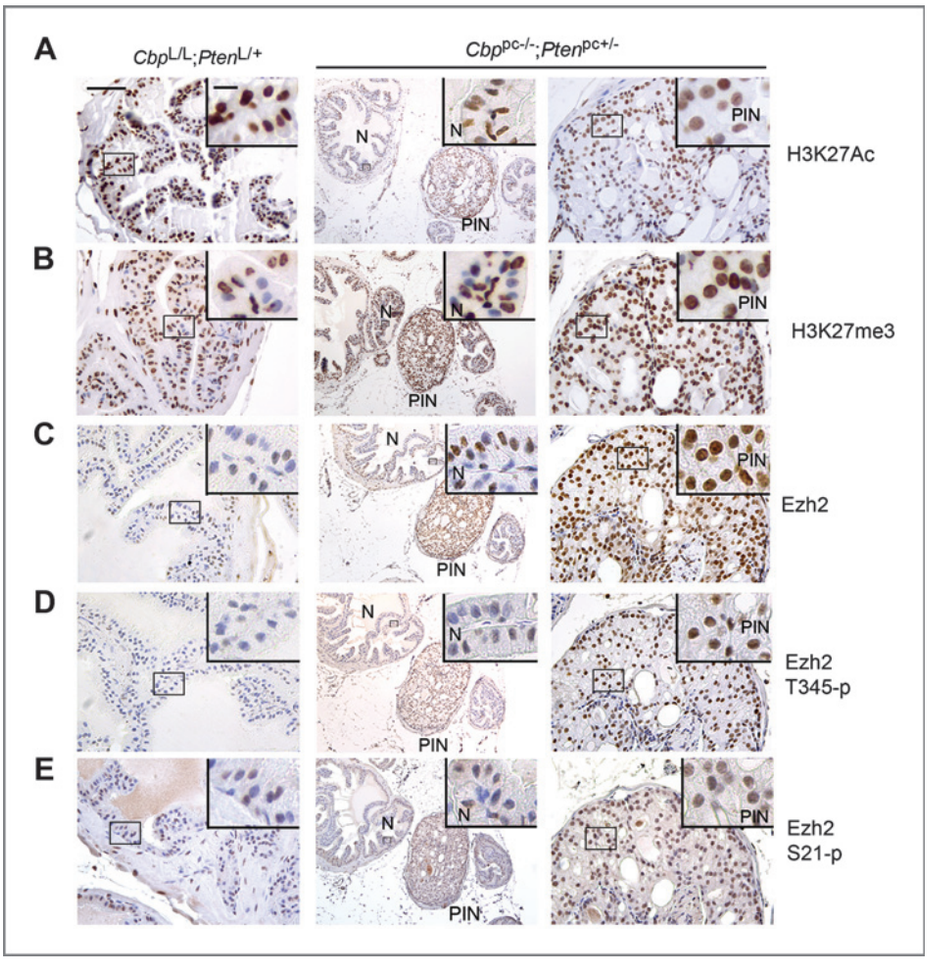

Figure 6. Immunohistochemical analysis of H3K27Ac, H3K27me3 and total, T345- and S21-phosphorylated Ezh2 in prostate sections of *Cbp*/*Pten*-deficient mice ($Cbp^{pc-/-}$;$Pten^{pc+/-}$) and "wild-type" littermate controls ($Cbp^{L/L}$;$Pten^{L/+}$). Prostate sections of 6-month-old mice were used for immunohistochemical analysis of expression of H3K27Ac (A), H3K27me3 (B), total Ezh2 (C), T345-phosphorylated Ezh2 (D), and S21-phosphorylated Ezh2 (E). Scale bar, 50 μm. Insets show high magnification images; scale bar, 10 μm. N, normal; PIN, prostatic intraepithelial neoplasia.

in expression of genes involved in apoptotic signaling pathways, including downregulation of the antiapoptotic proteins XIAP and BCL-xL and cleavage of caspase-3 and PARP (Supplementary Fig. S12A–S12C). Thus, the HDAC inhibitor LBH589 induces regression of PIN lesions in $Cbp^{pc-/-}$;$Pten^{pc+/-}$ mice via both inhibition of cell proliferation and induction of apoptosis.

Discussion

CBP is implicated in human cancers (10, 11), but its precise role in prostate oncogenesis remains elusive. For the first time, we provide *in vivo* evidence that *Cbp* deletion induces high-grade PIN/low-grade cancer in the mouse prostate in a *Pten* heterozygous background. We further demonstrate that reduced expression of CBP correlates with decreased expression of PTEN in a cohort of human prostate cancer specimens. Thus, we have established a clinically relevant mouse model that recapitulates the pathogenesis of early-stage prostate cancer.

Genome-wide analyses show that histone acetylation generally correlates with gene activation (7). CBP mediates H3K27Ac in mammals and flies (8, 9), whereas EZH2 promotes H3K27me3 (29). In line with the fact that H3K27Ac and H3K27me3 modifications occur on the same lysine, CBP antagonizes PcG protein-mediated gene silencing in *Drosophila* (8). We demonstrated for the first time in mammalian cells that codepletion of CBP and PTEN induces an H3K37Ac-to-H3K27me3 switch in bulk histones. This observation is substantiated by our finding that PTEN inactivation results in EZH2 activation by increasing expression of total and T350-phosphorylated EZH2 in MEF, human prostate cancer cell lines, and in the mouse prostate. These findings support a model (Fig. 7F) wherein deletion of CBP alone reduces H3K27Ac levels at EZH2 target gene loci and compromises their expression. Upregulation of EZH2 protein and function (via T350 phosphorylation) due to PTEN inactivation increases the level of the H3K27me3 histone mark, which further reduces or completely shuts off the expression of EZH2 target genes, thereby favoring tumor formation. This model is further validated by the observation that expression of EZH2 target genes is downregulated owe to CBP and/or PTEN codepletion. The coordinative effect of CBP loss and EZH2 activation on gene repression triggered by PTEN loss provides a plausible explanation as to why CBP deletion alone is insufficient to induce neoplastic changes in the prostate. Given that inactivation mutations of *CBP* gene are frequently detected in human

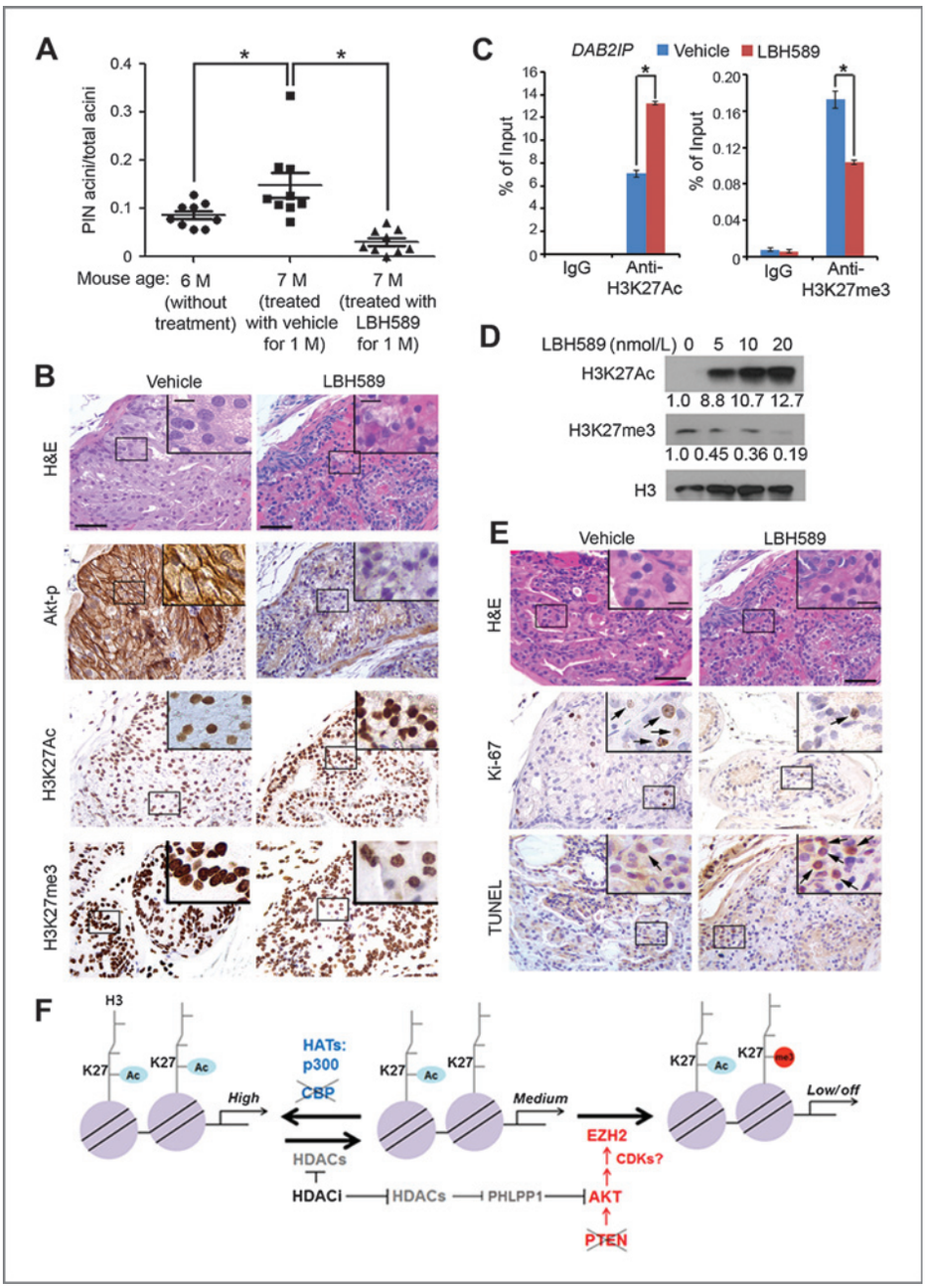

Figure 7. Histone deacetylase inhibitor panobinostat (LBH589) induces tumor repression, cell proliferation inhibition, and apoptosis in *Cbp*$^{pc-/-}$;*Pten*$^{pc+/-}$ mice. A, 6-month-old *Cbp*$^{pc-/-}$;*Pten*$^{pc+/-}$ mice ($n = 9$ per group) were sacrificed (column 1) or treated with vehicle or LBH589 (20 mg/kg/d) for 1 month and then sacrificed (columns 2 and 3). Prostate tissues were harvested, sectioned, and H&E stained. Sections with comparable acini numbers in each group were examined for PIN acini. The data were obtained in a blinded fashion. M, month. *, $P < 0.05$. B, histologic and immunohistochemical analysis of Akt-p, H3K27Ac, and H3K27me3 in prostate sections of mice treated with vehicle or LBH589. Scale bar, 50 μm. Insets show high magnification images; scale bar, 10 μm. C, effect of LBH589 on H3K27Ac and H3K27me3 levels at the *DAB2IP* gene locus in PTEN/CBP knockdown DU145 cells. Cells were transfected with CBP and PTEN-specific siRNAs for 24 hours and treated with 20 nmol/L LBH589 for 24 hours followed by ChIP analysis with H3K27Ac and H3K27me3 antibodies. Enrichment of H3K27Ac and H3K27me3 was determined by ChIP-qPCR ($n = 3$). *, $P < 0.01$. D, effect of LBH589 on expression of H3K27Ac and H3K27me3 of bulk histones in PTEN/CBP knockdown DU145 cells. Cells were transfected as in C for 24 hours, treated with LBH589 at different doses (5, 10, 20 nmol/L) for 24 hours followed by Western blot analysis. The density of H3K27Ac and H3K27me3 was determined by normalizing to H3 first and then to the normalized value in mock-treated cells. E, Ki-67 staining and TUNEL assay were performed on prostate sections obtained from mice used in experiments as described in A. Scale bar, 50 μm. Insets show high magnification images; scale bar, 10 μm. F, diagram deciphering the synergistic effect of CBP and PTEN codeficiency on the H3K27Ac-to-H3K27me3 switch on chromatin and their impact on gene expression. Light purple circles represent nucleosomes.

recurrent lymphomas and small-cell lung cancers (10, 11, 42), it is possible that like in the prostate, CBP, a generic histone acetyltransferase (6) may act as a tumor suppressor in a context-dependent manner in those types of tissues.

Besides its overexpression in metastatic prostate cancer, EZH2 was found significantly upregulated in benign prostatic hyperplasia and primary prostate cancer (43). EZH2 overexpression in early lesions such as PIN is also observed in *Pten*-knockout mice (34). Thus, in addition to its role in late-stage castration-resistant prostate cancer (37), there is ample evidence suggesting that deregulated EZH2 also plays a pivotal role in the early-stage pathogenesis of prostate cancer. This notion is fully supported by our model wherein EZH2 is crucial for *Cbp*/*Pten* deletion-induced tumorigenesis in the prostate (Fig. 7F).

AKT is invariably activated in PTEN-null prostate cancer (15). Transgenic expression of constitutively active AKT alone induces PIN in the mouse prostate (44), suggesting that AKT activation itself is sufficient to drive prostate epithelial cell transformation and early-stage prostate cancer pathogenesis. The finding in mouse models is substantiated by the observation that AKT phosphorylation is significantly elevated at human PIN (45). Intriguingly, we found that Akt is highly phosphorylated in PIN, but not in the adjacent nonmalignant prostatic epithelial cells in $Cbp^{pc-/-}$;$Pten^{pc+/-}$ mice and in the prostatic epithelium in "wild-type" mice. Thus, homozygous *Cbp* deletion in *Pten* heterozygous background predisposes the prostatic epithelium for secondary genetic and/or epigenetic lesions, which may in turn lead to Akt activation and prostate tumorigenesis. Further analysis is warranted to define the molecular basis underlying Akt activation in PIN lesions in *Cbp*/*Pten* compound-deficient mice.

An early study demonstrates that AKT phosphorylates EZH2 at S21 and inhibits EZH2's H3K27me3 activity (36). An independent study reports that T350 but not S21 phosphorylation was readily detected by mass spectrometry in 293T cells (30), suggesting that the overall level of S21 phosphorylation may be lower than T350 phosphorylation in these cells. Moreover, it has been shown recently that although both androgen-sensitive LNCaP and castration-resistant abl prostate cancer cells are PTEN-negative, surprisingly, EZH2 S21 phosphorylation was barely detected in LNCaP but was much higher in abl (37), implying that in addition to PTEN loss, other defects are essential for AKT-mediated S21 phosphorylation in prostate cancer cells. Indeed, besides PTEN loss, AKT is hyperactivated due to decreased expression of the AKT phosphatase PHLPP1 and the impaired FKBP51-PHLPP1 complex in abl cells under androgen depletion conditions (34, 37). In agreement with the findings from these studies, we found that although Akt was activated in PIN in non-castrated *Cbp*/*Pten* knockout mice (Fig. 4D), only very modest S21 phosphorylation of Ezh2 was detected in these tissues (Fig. 6E). In contrast, both total Ezh2 and T350 phosphorylation, an indicator of Ezh2 activation (19, 30, 31), was substantially upregulated (Fig. 6C and D), which is consistent with high levels of H3K27me3 in these tissues (Fig. 6B and Supplementary Fig. S10). Based upon the findings from our mouse model and others from human prostate cancers and cell lines (37), it can be postulated that S21 phosphorylation-mediated inhibitory effect on EZH2's H3K27me3 activity is minimal in uncastrated PTEN-deficient prostate tumors like those in *Cbp*/*Pten* deletion mice. In castration-resistant prostate cancer, however, the H3K27me3-dependent Polycomb function of EZH2 may be mitigated due to aberrant activation of AKT and subsequent S21 hyperphosphorylation of EZH2 (37).

A pilot phase I clinical study showed that the anticancer effect of oral panobinostat (LBH589) on castration-resistant prostate cancer was not quite promising, even though increased histone acetylation was observed in peripheral blood mononuclear cells (40), suggesting that new biomarkers are needed to identify patients with prostate cancer who are responsive to HDAC inhibitors. Inactivation mutations in the *CBP* gene frequently recur in relapsed lymphoblastic leukemia and B-cell lymphoma (10, 11) and that *Cbp* deletion induces T-cell lymphoma in mice (12). Notably, patients with lymphoma respond favorably to the HDAC inhibitor. In a striking similarity, we demonstrated that both CBP and PTEN protein expression is downregulated in a large cohort of human prostate cancer samples and that LBH589 treatment induces regression of *Cbp*/*Pten*-deficient PIN in mice. Our findings suggest that CBP- and PTEN-deficient prostate cancer patients may be susceptible to the HDAC inhibitory drugs (Fig. 7F).

In summary, we demonstrate that concomitant deletion of two *Cbp* alleles and one *Pten* allele induces early-life high-grade PIN/low-grade cancer in the mouse prostate. Of note, whether PTEN is lost in human PIN lesions has recently been called into question (46), suggesting a potential weakness in our model. Nonetheless, we further show that codeficiency of CBP and PTEN increases cell proliferation, induces an acetylation-to-trimethylation shift on lysine 27 of pan histone H3, and causes transcriptional repression of DAB2IP and $p27^{KIP1}$ tumor suppressor proteins of EZH2 targets. Our model not only recapitulates the pathogenesis of early-stage prostate cancer, but also is highly clinically relevant as expression of CBP, PTEN, and $p27^{KIP1}$ correlates in human prostate cancer. Our finding that treatment of $Cbp^{pc-/-}$;$Pten^{pc+/-}$ mice with panobinostat induces regression of PIN implies that deregulated CBP and PTEN may serve as a biomarker for epigenetic-targeted therapy of human prostate cancers.

Disclosure of Potential Conflicts of Interest

No potential conflicts of interest were disclosed.

Authors' Contributions

Conception and design: L. Ding, S. Chen, J. Van Deursen, H. Huang
Development of methodology: L. Ding, S. Chen, P. Liu, A. Rizzardi, S.C. Schmechel, J. Van Deursen
Acquisition of data (provided animals, acquired and managed patients, provided facilities, etc.): L. Ding, S. Chen, J. Zhong, K.M. Regan, A. Rizzardi, L. Cheng, S.C. Schmechel, J.C. Cheville
Analysis and interpretation of data (e.g., statistical analysis, biostatistics, computational analysis): L. Ding, P. Liu, L. Wang, A. Rizzardi, L. Cheng, J. Zhang, J. Van Deursen, H. Huang
Writing, review, and/or revision of the manuscript: L. Ding, S. Chen, J. Zhong, A. Rizzardi, L. Cheng, S.C. Schmechel, J.C. Cheville, J. van Deursen, D.J. Tindall, H. Huang
Administrative, technical, or material support (i.e., reporting or organizing data, constructing databases): L. Ding, S. Chen, Y. Pan, C. Yu, A. Rizzardi, L. Cheng
Study supervision: C. Yu, J. Zhang, H. Huang

Grant Support

This work is supported in part by grants from the NIH (CA134514 and CA130908 to H. Huang; CA091956 to D.J. Tindall), the Department of Defense (W81XWH-09-1-622 and W81XWH-07-1-0137 to H. Huang) and the T.J. Martell Foundation.

The costs of publication of this article were defrayed in part by the payment of page charges. This article must therefore be hereby marked *advertisement* in accordance with 18 U.S.C. Section 1734 solely to indicate this fact.

Received June 12, 2013; revised January 23, 2014; accepted January 27, 2014; published OnlineFirst February 3, 2014.

References

1. Sakr WA, Grignon DJ, Crissman JD, Heilbrun LK, Cassin BJ, Pontes JJ, et al. High grade prostatic intraepithelial neoplasia (HGPIN) and prostatic adenocarcinoma between the ages of 20–69: an autopsy study of 249 cases. In Vivo 1994;8:439–43.
2. Deocampo ND, Huang H, Tindall DJ. The role of PTEN in the progression and survival of prostate cancer. Minerva Endocrinol 2003;28: 145–53.
3. McMenamin ME, Soung P, Perera S, Kaplan I, Loda M, Sellers WR. Loss of PTEN expression in paraffin-embedded primary prostate cancer correlates with high Gleason score and advanced stage. Cancer Res 1999;59:4291–6.
4. Di Cristofano A, De Acetis M, Koff A, Cordon-Cardo C, Pandolfi PP. Pten and p27KIP1 cooperate in prostate cancer tumor suppression in the mouse. Nat Genet 2001;27:222–4.
5. King JC, Xu J, Wongvipat J, Hieronymus H, Carver BS, Leung DH, et al. Cooperativity of TMPRSS2-ERG with PI3-kinase pathway activation in prostate oncogenesis. Nat Genet 2009;41:524–6.
6. Goodman RH, Smolik S. CBP/p300 in cell growth, transformation, and development. Genes Dev 2000;14:1553–77.
7. Wang Z, Zang C, Rosenfeld JA, Schones DE, Barski A, Cuddapah S, et al. Combinatorial patterns of histone acetylations and methylations in the human genome. Nat Genet 2008;40:897–903.
8. Tie F, Banerjee R, Stratton CA, Prasad-Sinha J, Stepanik V, Zlobin A, et al. CBP-mediated acetylation of histone H3 lysine 27 antagonizes Drosophila Polycomb silencing. Development 2009;136:3131–41.
9. Jin Q, Yu LR, Wang L, Zhang Z, Kasper LH, Lee JE, et al. Distinct roles of GCN5/PCAF-mediated H3K9ac and CBP/p300-mediated H3K18/27ac in nuclear receptor transactivation. EMBO J 2011;30:249–62.
10. Mullighan CG, Zhang J, Kasper LH, Lerach S, Payne-Turner D, Phillips LA, et al. CREBBP mutations in relapsed acute lymphoblastic leukaemia. Nature 2011;471:235–9.
11. Pasqualucci L, Dominguez-Sola D, Chiarenza A, Fabbri G, Grunn A, Trifonov V, et al. Inactivating mutations of acetyltransferase genes in B-cell lymphoma. Nature 2011;471:189–95.
12. Kang-Decker N, Tong C, Boussouar F, Baker DJ, Xu W, Leontovich AA, et al. Loss of CBP causes T cell lymphomagenesis in synergy with p27Kip1 insufficiency. Cancer Cell 2004;5:177–89.
13. Tillinghast GW, Partee J, Albert P, Kelley JM, Burtow KH, Kelly K. Analysis of genetic stability at the EP300 and CREBBP loci in a panel of cancer cell lines. Genes Chromosomes Cancer 2003;37: 121–31.
14. So CK, Nie Y, Song Y, Yang GY, Chen S, Wei C, et al. Loss of heterozygosity and internal tandem duplication mutations of the CBP gene are frequent events in human esophageal squamous cell carcinoma. Clin Cancer Res 2004;10:19–27.
15. Wang S, Gao J, Lei Q, Rozengurt N, Pritchard C, Jiao J, et al. Prostate-specific deletion of the murine Pten tumor suppressor gene leads to metastatic prostate cancer. Cancer Cell 2003;4:209–21.
16. Wu X, Wu J, Huang J, Powell WC, Zhang J, Matusik RJ, et al. Generation of a prostate epithelial cell-specific Cre transgenic mouse model for tissue-specific gene ablation. Mech Dev 2001;101:61–9.
17. Lesche R, Groszer M, Gao J, Wang Y, Messing A, Sun H, et al. Cre/loxP-mediated inactivation of the murine Pten tumor suppressor gene. Genesis 2002;32:148–9.
18. Chen Z, Trotman LC, Shaffer D, Lin HK, Dotan ZA, Niki M, et al. Crucial role of p53-dependent cellular senescence in suppression of Pten-deficient tumorigenesis. Nature 2005;436:725–30.
19. Chen S, Bohrer LR, Rai AN, Pan Y, Gan L, Zhou X, et al. Cyclin-dependent kinases regulate epigenetic gene silencing through phosphorylation of EZH2. Nat Cell Biol 2010;12:1108–14.
20. Linja MJ, Porkka KP, Kang Z, Savinainen KJ, Janne OA, Tammela TL, et al. Expression of androgen receptor coregulators in prostate cancer. Clin Cancer Res 2004;10:1032–40.
21. Comuzzi B, Lambrinidis L, Rogatsch H, Godoy-Tundidor S, Knezevic N, Krhen I, et al. The transcriptional co-activator cAMP response element-binding protein-binding protein is expressed in prostate cancer and enhances androgen- and anti-androgen-induced androgen receptor function. Am J Pathol 2003;162:233–41.
22. Suzuki H, Freije D, Nusskern DR, Okami K, Cairns P, Sidransky D, et al. Interfocal heterogeneity of PTEN/MMAC1 gene alterations in multiple metastatic prostate cancer tissues. Cancer Res 1998;58:204–9.
23. Gao H, Ouyang X, Banach-Petrosky WA, Shen MM, Abate-Shen C. Emergence of androgen independence at early stages of prostate cancer progression in Nkx3.1; Pten mice. Cancer Res 2006;66: 7929–33.
24. Chen H, Pong RC, Wang Z, Hsieh JT. Differential regulation of the human gene DAB2IP in normal and malignant prostatic epithelia: cloning and characterization. Genomics 2002;79:573–81.
25. Wang Z, Tseng CP, Pong RC, Chen H, McConnell JD, Navone N, et al. The mechanism of growth-inhibitory effect of DOC-2/DAB2 in prostate cancer. Characterization of a novel GTPase-activating protein associated with N-terminal domain of DOC-2/DAB2. J Biol Chem 2002; 277:12622–31.
26. Cheville JC, Lloyd RV, Sebo TJ, Cheng L, Erickson L, Bostwick DG, et al. Expression of p27kip1 in prostatic adenocarcinoma. Mod Pathol 1998;11:324–8.
27. O'Meara MM, Simon JA. Inner workings and regulatory inputs that control Polycomb repressive complex 2. Chromosoma 2012;121: 221–34.
28. Pasini D, Malatesta M, Jung HR, Walfridsson J, Willer A, Olsson L, et al. Characterization of an antagonistic switch between histone H3 lysine 27 methylation and acetylation in the transcriptional regulation of Polycomb group target genes. Nucleic Acids Res 2010;38: 4958–69.
29. Cao R, Wang L, Wang H, Xia L, Erdjument-Bromage H, Tempst P, et al. Role of histone H3 lysine 27 methylation in Polycomb-group silencing. Science 2002;298:1039–43.
30. Kaneko S, Li G, Son J, Xu CF, Margueron R, Neubert TA, et al. Phosphorylation of the PRC2 component Ezh2 is cell cycle-regulated and up-regulates its binding to ncRNA. Genes Dev 2010;24: 2615–20.
31. Wu SC, Zhang Y. Cyclin-dependent kinase 1 (CDK1)-mediated phosphorylation of enhancer of zeste 2 (Ezh2) regulates its stability. J Biol Chem 2011;286:28511–9.
32. Sun H, Lesche R, Li DM, Liliental J, Zhang H, Gao J, et al. PTEN modulates cell cycle progression and cell survival by regulating phosphatidylinositol 3,4,5,-trisphosphate and Akt/protein kinase B signaling pathway. Proc Natl Acad Sci U S A 1999;96:6199–204.
33. Kuzmichev A, Margueron R, Vaquero A, Preissner TS, Scher M, Kirmizis A, et al. Composition and histone substrates of polycomb repressive group complexes change during cellular differentiation. Proc Natl Acad Sci U S A 2005;102:1859–64.
34. Mulholland DJ, Tran LM, Li Y, Cai H, Morim A, Wang S, et al. Cell autonomous role of PTEN in regulating castration-resistant prostate cancer growth. Cancer Cell 2011;19:792–804.
35. Wang L, Zeng X, Chen S, Ding L, Zhong J, Zhao JC, et al. BRCA1 is a negative modulator of the PRC2 complex. EMBO J 2013;32:1584–97.
36. Cha TL, Zhou BP, Xia W, Wu Y, Yang CC, Chen CT, et al. Akt-mediated phosphorylation of EZH2 suppresses methylation of lysine 27 in histone H3. Science 2005;310:306–10.

37. Xu K, Wu ZJ, Groner AC, He HH, Cai C, Lis RT, et al. EZH2 oncogenic activity in castration-resistant prostate cancer cells is Polycomb-independent. Science 2012;338:1465–9.
38. Gupta M, Ansell SM, Novak AJ, Kumar S, Kaufmann SH, Witzig TE. Inhibition of histone deacetylase overcomes rapamycin-mediated resistance in diffuse large B-cell lymphoma by inhibiting Akt signaling through mTORC2. Blood 2009;114:2926–35.
39. Giles F, Fischer T, Cortes J, Garcia-Manero G, Beck J, Ravandi F, et al. A phase I study of intravenous LBH589, a novel cinnamic hydroxamic acid analogue histone deacetylase inhibitor, in patients with refractory hematologic malignancies. Clin Cancer Res 2006;12:4628–35.
40. Rathkopf D, Wong BY, Ross RW, Anand A, Tanaka E, Woo MM, et al. A phase I study of oral panobinostat alone and in combination with docetaxel in patients with castration-resistant prostate cancer. Cancer Chemother Pharmacol 2010;66:181–9.
41. Bradley EW, Carpio LR, Westendorf JJ. Histone deacetylase 3 suppression increases PH domain and leucine-rich repeat phosphatase (Phlpp)1 expression in chondrocytes to suppress Akt signaling and matrix secretion. J Biol Chem 2013;288:9572–82.
42. Peifer M, Fernandez-Cuesta L, Sos ML, George J, Seidel D, Kasper LH, et al. Integrative genome analyses identify key somatic driver mutations of small-cell lung cancer. Nat Genet 2012;44:1104–10.
43. Varambally S, Dhanasekaran SM, Zhou M, Barrette TR, Kumar-Sinha C, Sanda MG, et al. The polycomb group protein EZH2 is involved in progression of prostate cancer. Nature 2002;419:624–9.
44. Majumder PK, Yeh JJ, George DJ, Febbo PG, Kum J, Xue Q, et al. Prostate intraepithelial neoplasia induced by prostate restricted Akt activation: the MPAKT model. Proc Natl Acad Sci U S A 2003;100:7841–6.
45. Paweletz CP, Charboneau L, Bichsel VE, Simone NL, Chen T, Gillespie JW, et al. Reverse phase protein microarrays which capture disease progression show activation of pro-survival pathways at the cancer invasion front. Oncogene 2001;20:1981–9.
46. Lotan TL, Gumuskaya B, Rahimi H, Hicks JL, Iwata T, Robinson BD, et al. Cytoplasmic PTEN protein loss distinguishes intraductal carcinoma of the prostate from high-grade prostatic intraepithelial neoplasia. Mod Pathol 2013;26:587–603.